Supplementary Fig.1

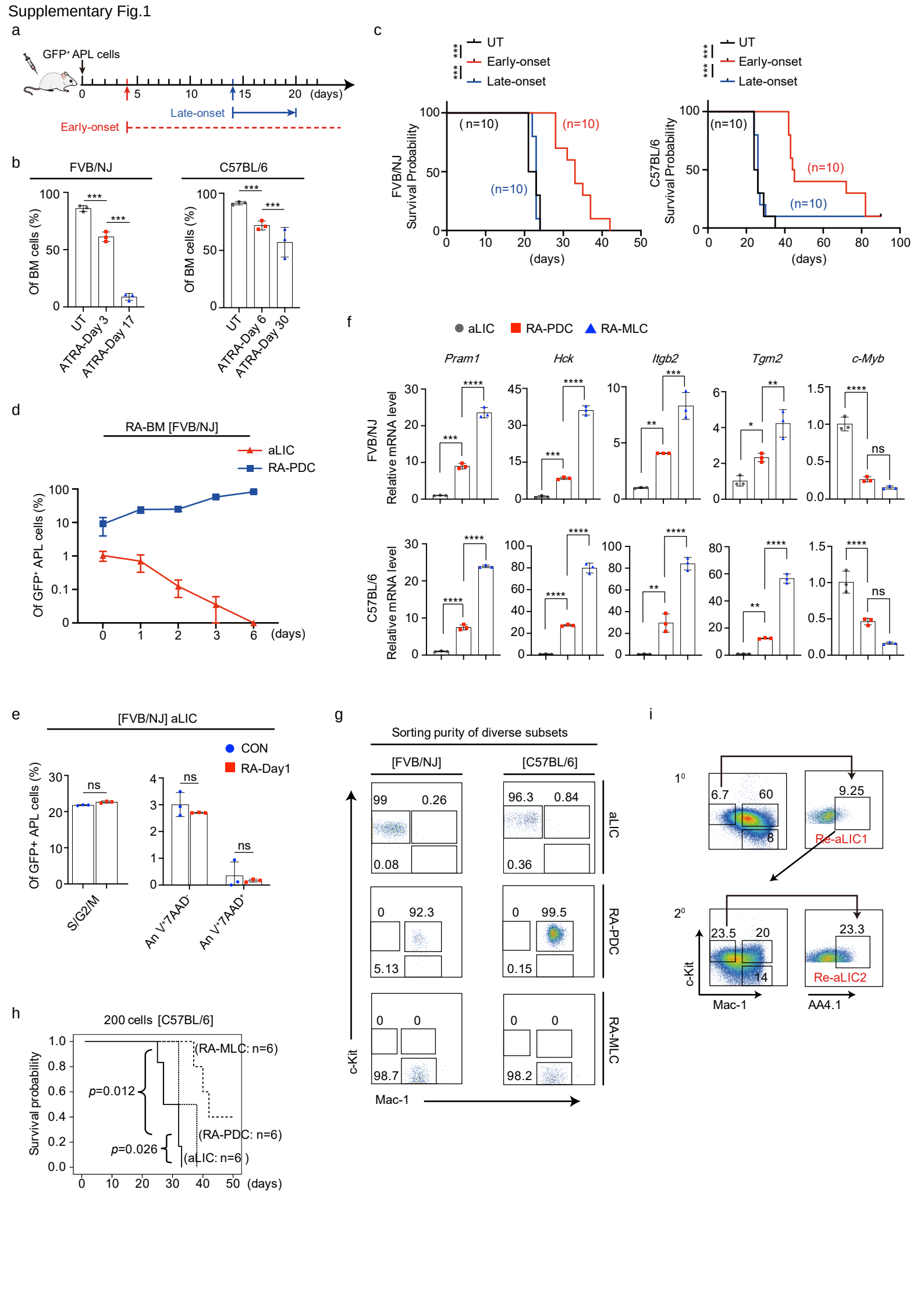

Supplementary Fig.1 ATRA-induced partially differentiated APL cells possess de-differentiation potential, related to Fig.1.

(a) Schematic diagram of the experimental plan. Intraperitoneal injection of ATRA (10 mg/kg) was started on day 4 (when GFP^+ leukemia cells in PBL were undetectable, early-onset) or day 14 (when GFP^+ leukemia cells were approximately 1% of PBL, late-onset) after the inoculation of 5,000 APL cells into FVB/NJ or C57BL/6 recipients. UT: untreated.

(b) After ATRA treatment for the indicated periods, the percentages of GFP^+ APL cells within the BM were measured by flow cytometry. UT: untreated.

(c) Survival curves of the FVB/NJ or C57BL/6 leukemic recipients treated with an early-onset or late-onset ATRA regimen (n=10). UT: untreated.

(d) The dynamic frequency alterations of aLICs and RA-PDCs/PDCs within the BM GFP^+ leukemic population after treatment with ATRA for 1, 2, 3, and 6 days.

(**e**) At the overt leukemic phase (FVB/NJ model), the recipients were treated with or without ATRA for 1 day, and the gated c-$Kit^+$$Mac\text{-}1^-$$AA4.1^+$ cells from BM GFP^+ APL section were analyzed. Annexin V and 7-AAD staining for cell survival, and Hochest 33342 and Ki67 staining for cell cycle status.

(f) Real-time PCR assay for the expression levels of PML/RARα-regulated genes and LSC signature gene as indicated in aLICs, RA-PDCs and RA-MLCs isolated from FVB/NJ and C57BL/6 models, respectively.

(g) A representative flow cytometric analysis of the sorting purity of the indicated leukemic subsets.

(h) The survival curves of different groups of C57BL/6 recipients that received 200 aLICs, RA-PDCs or RA-MLCs were isolated from the C57BL/6 models that had been treated with ATRA for 6 days.

(i) Relative distribution of aLICs, PDCs and MLCs within the BM of syngeneic recipients (1^0) inoculated with 1-5 RA-PDCs. The regenerated aLICs initiated full-scale leukemia in the secondary recipients (2^0).

Data are presented as mean ± SD. *p<0.05, **p<0.01, ***p<0.001. ns: not significant.

Supplementary Fig.2

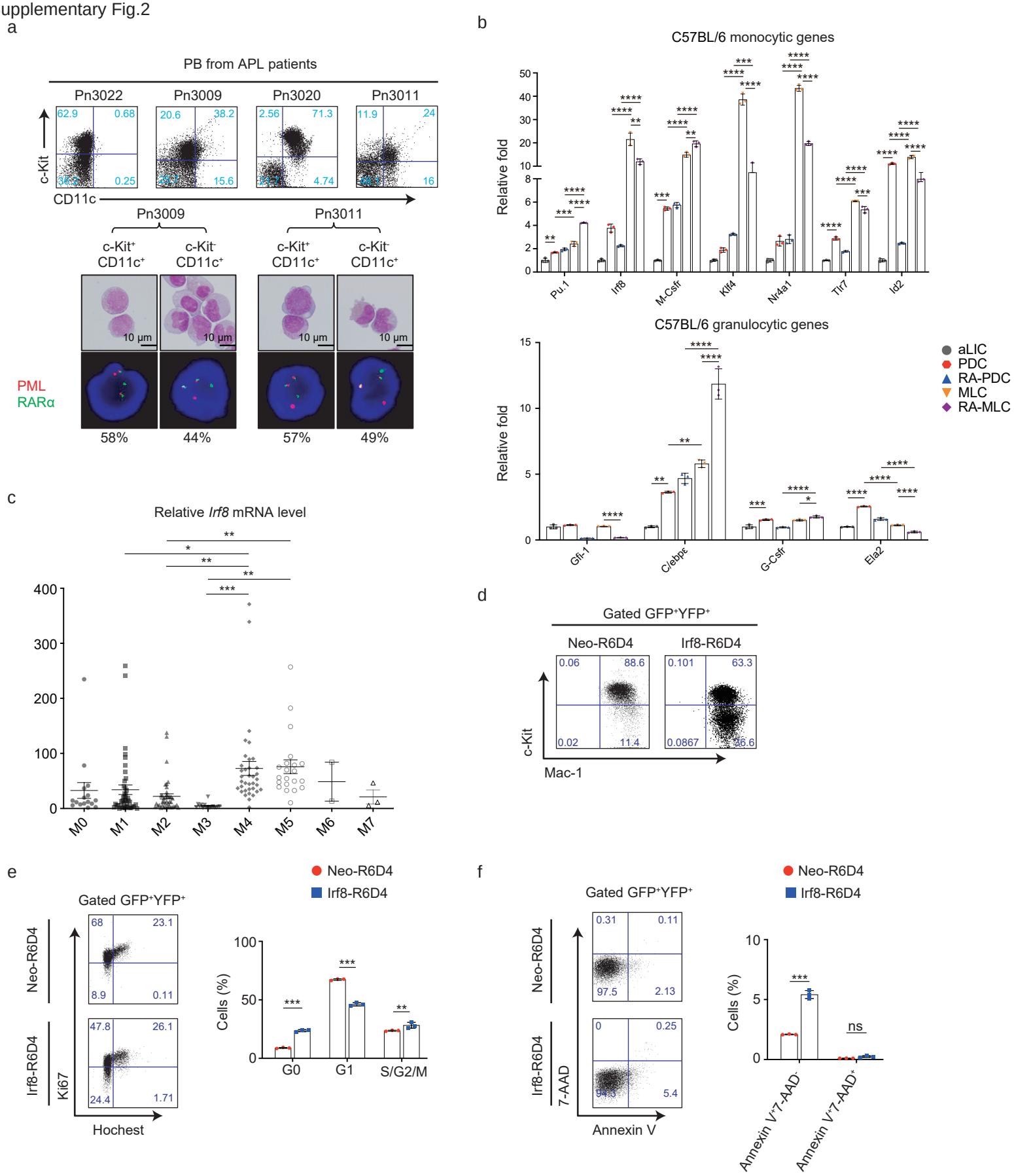

Supplementary Fig.2 Human and mouse APL cells harbor spontaneous monocytic differentiation potential, related to Fig.2.

(a) FACS-sorted c-Kit$^-$CD11c$^+$ or c-Kit$^+$CD11c$^+$ PBMCs from APL patients were tested for fluorescence in situ hybridization (FISH) of t (15;17). Pn: patient number.

(b) RT-PCR assay for mRNA levels of representative monocytic (upper) and granulocytic (bottom) genes in the cellular subsets as indicated from the C57BL/6 models.

(c) Expression profile of *irf8* mRNA across eight human AML subtypes using raw data from the TCGA-LAML dataset.M0, n=16; M1, n=42; M2, n=41; M3, n=16; M4, n=36; M5, n=21; M6, n=2; M7, n=3. Pairwise comparisons were performed between M3 and each one of the other subtypes.

(d-f) FVB/NJ mice intravenously implanted with 2×10^5 Neo- or Irf8-GFP$^+$YFP$^+$ leukemia cells were treated with the R6D4 regimen. Flow cytometric analysis showed the percentages of aLICs, PDCs, and MLCs among GFP$^+$YFP$^+$ cellular sections **(d)**, their cell-cycle status **(e)** and Annexin V and 7-AAD staining for cell survival **(f)**. Data are presented as mean ± SD. *p<0.05, **p<0.01, ***p<0.001. ns: not significant.

Supplementary Fig.3

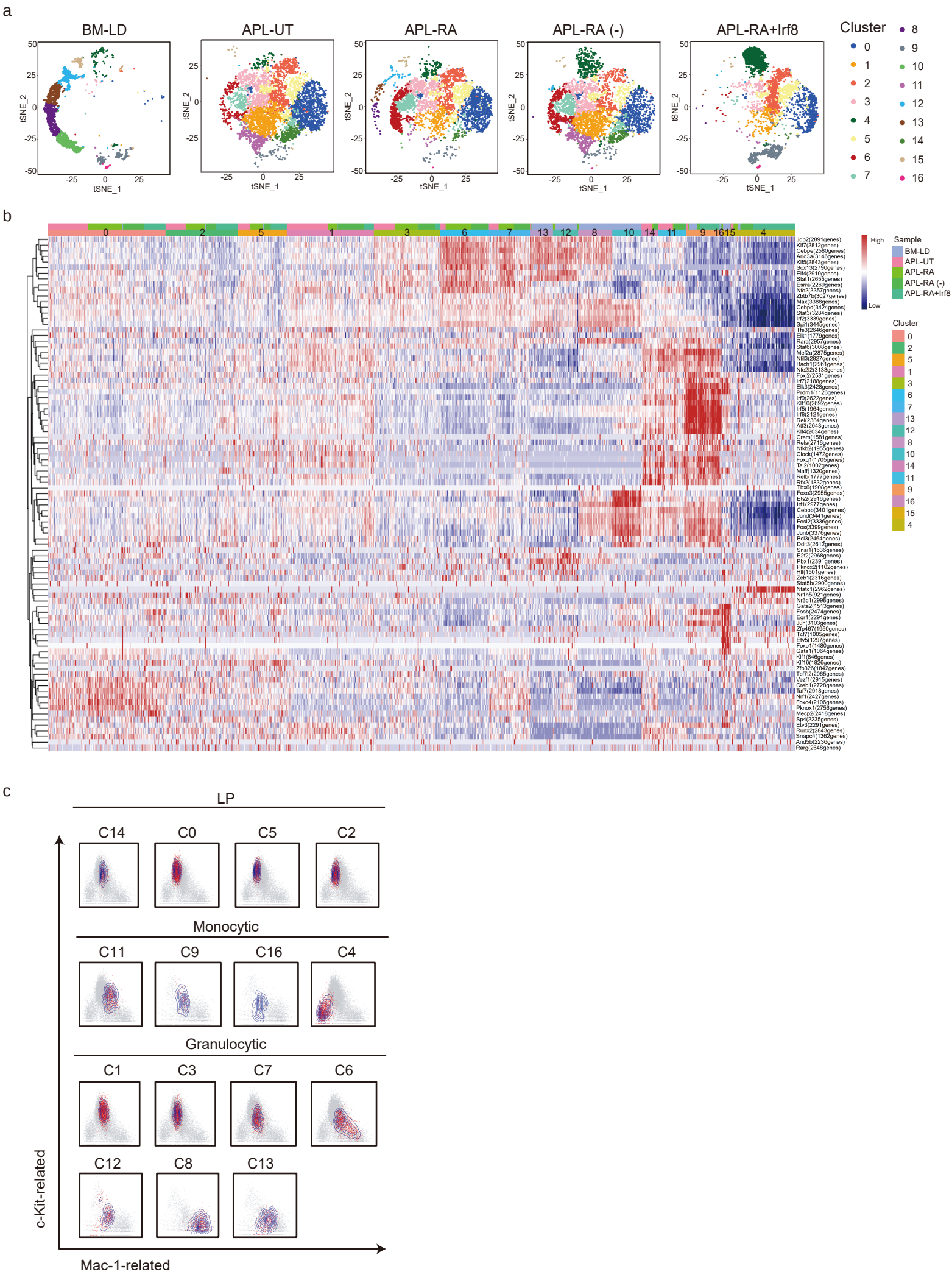

Supplementary Fig.3 Characterization of the APL hierarchy with scRNA-seq analysis, related to Fig.3.

(a) The t-Stochastic Neighbor Embedding (t-SNE) plot of specific combinations of cellular clusters for each of the 5 samples.

(b) Heatmap showing the differential expression patterns of cluster-discriminating marker genes.

(c) The contour lines are obtained by averaging the normalized expression levels of the c-Kit-related stemness module and Mac-1-related differentiation module in each cluster.

Data are presented as mean ± SD. *p<0.05, **p<0.01, ***p<0.001. ns: not significant.

Supplementary Fig.4

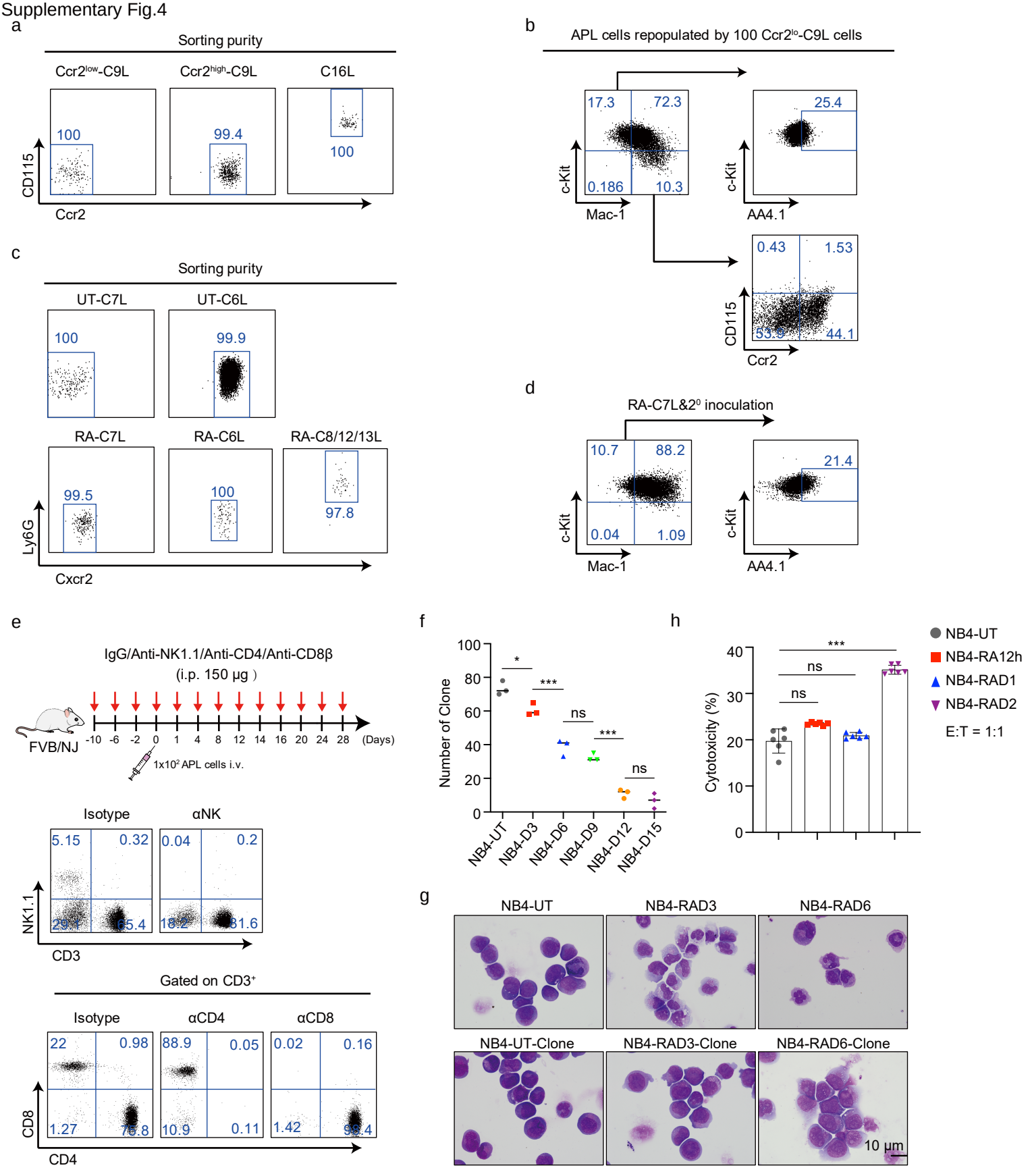

Supplementary Fig.4 ATRA sensitizes late granulocytic LICs to NK cells-mediated immune rejection, related to Fig.4.

(a) Flow cytometric examination of the sorting purity of RA/Irf8-induced CCR2^{lo}-C9L, CCR2^{hi}-C9, and C16L cells.

(b) Flow cytometry analysis of leukemic hierarchy re-established by inoculation of 100 RA/Irf8-induced Ccr2^{lo}-C9L cells.

(c) Flow cytometric examination of the sorting purity of UT-C7L, UT-C6L, RA-C7L, RA-C6L, and RA-C8/12/13L cells.

(d) Flow cytometry analysis of leukemic hierarchy re-established by inoculation of 100 RA-C7L cells into FVB/NJ recipients.

(e) Overview of the immune cell depletion study. Anti-NK1.1, anti-CD4, anti-CD8 (150 μg/each mouse, 3 times/week, i.p.) or antibody isotype IgG control were injected into 6-8-weeks-old FVB/NJ mice (n=5 for each group) at indicated time points (left panel). Representative flow cytometric analyses of indicated NK, CD4$^+$ or CD8$^+$ T cells in peripheral blood on day 0 are shown in the right panel.

(f,g) Human APL NB4 cells were treated with ATRA for the indicated times, and the retrieved cells were inoculated into 96-well plates with fresh conditioned medium (CM) at density of 1 cell/well. The clone-forming number was counted (**f**), and the Wright-Giemsa staining of UT-NB4, NB4-RAD3, and NB4-RAD6 cells (upper panel) and corresponding reformed clonal cells (bottom panel) are shown on (**g**).

(h) NB4 cells with or without RA treatment were tested for their susceptibility to NK92 cell-mediated killing (E:T=1:1), and apoptosis analysis was conducted 24 hours later.

Data are presented as mean ± SD. *p<0.05, **p<0.01, ***p<0.001. ns: not significant.

Supplementary Fig.5

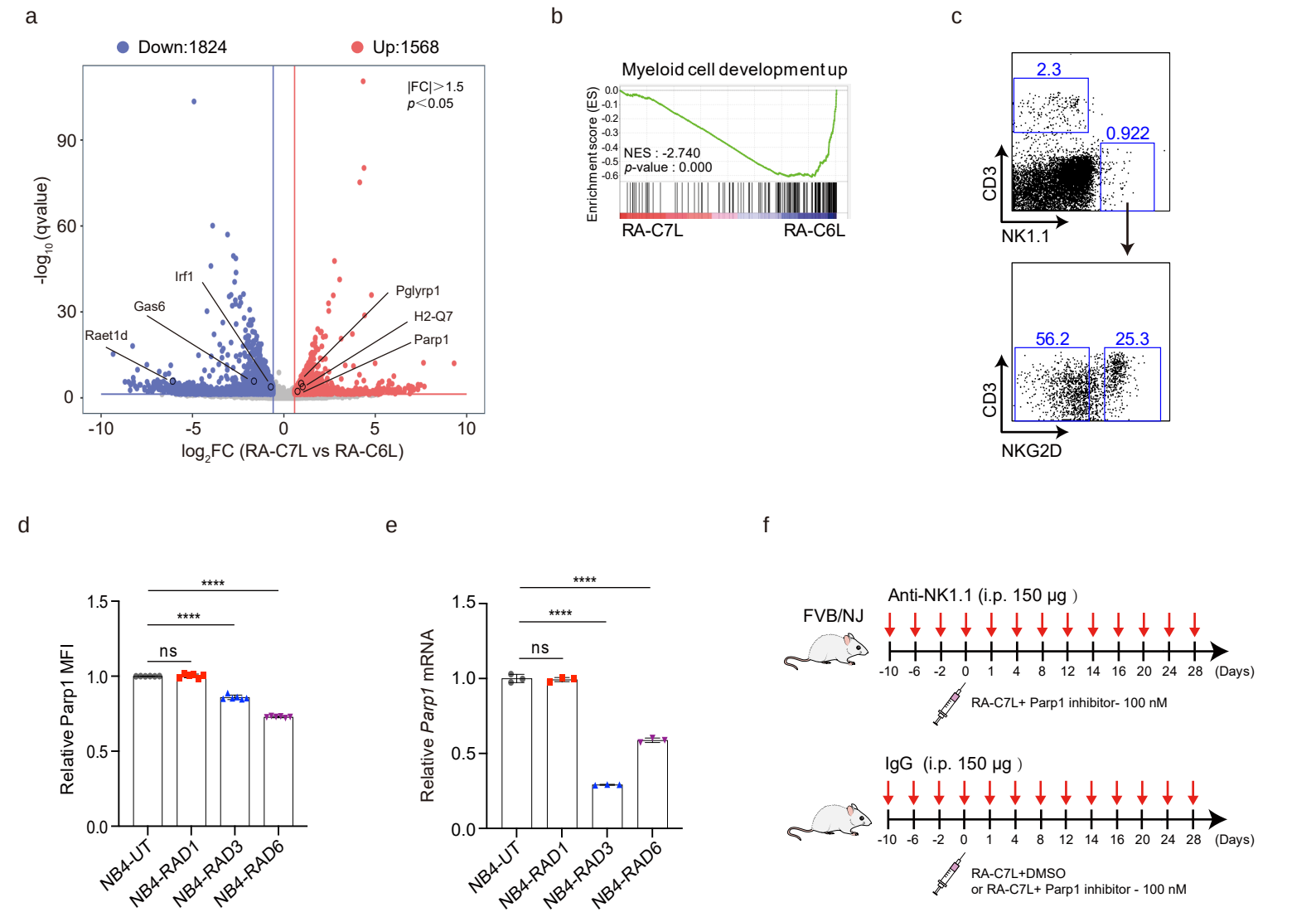

Supplementary Fig.5 ATRA upregulates the expression of Raet-1 during RA-C7L to RA-C6L differentiation, related to Fig.5.

(**a**) Volcano plot showing the enrichment profile of differentially expressed genes between RA-C7L and RA-C6L cells.

(**b**) GSEA of the myeloid cell differentiation-associated signature between RA-C7L and RA-C6L cells.

(**c**) Flow cytometry-defined expression of Parp1 on NB4 cells that were treated with ATRA for the indicated times.

(**d**) Real-time PCR assay for the expression levels of Parp1 in the NB4 cells that were treated with ATRA for the indicated times.

(**e**) Overview of the study (**Fig 5f**). Anti-NK1.1 (150 μg/each mouse, 3 times/week, i.p.) or isotype IgG control were injected into FVB/NJ mice (n=10 for each group) at indicated time points. RA-C7L cells were treated with 10nM Talazoparib or DMSO for 24 hours *in vitro* before inoculation.

Supplementary Fig.6

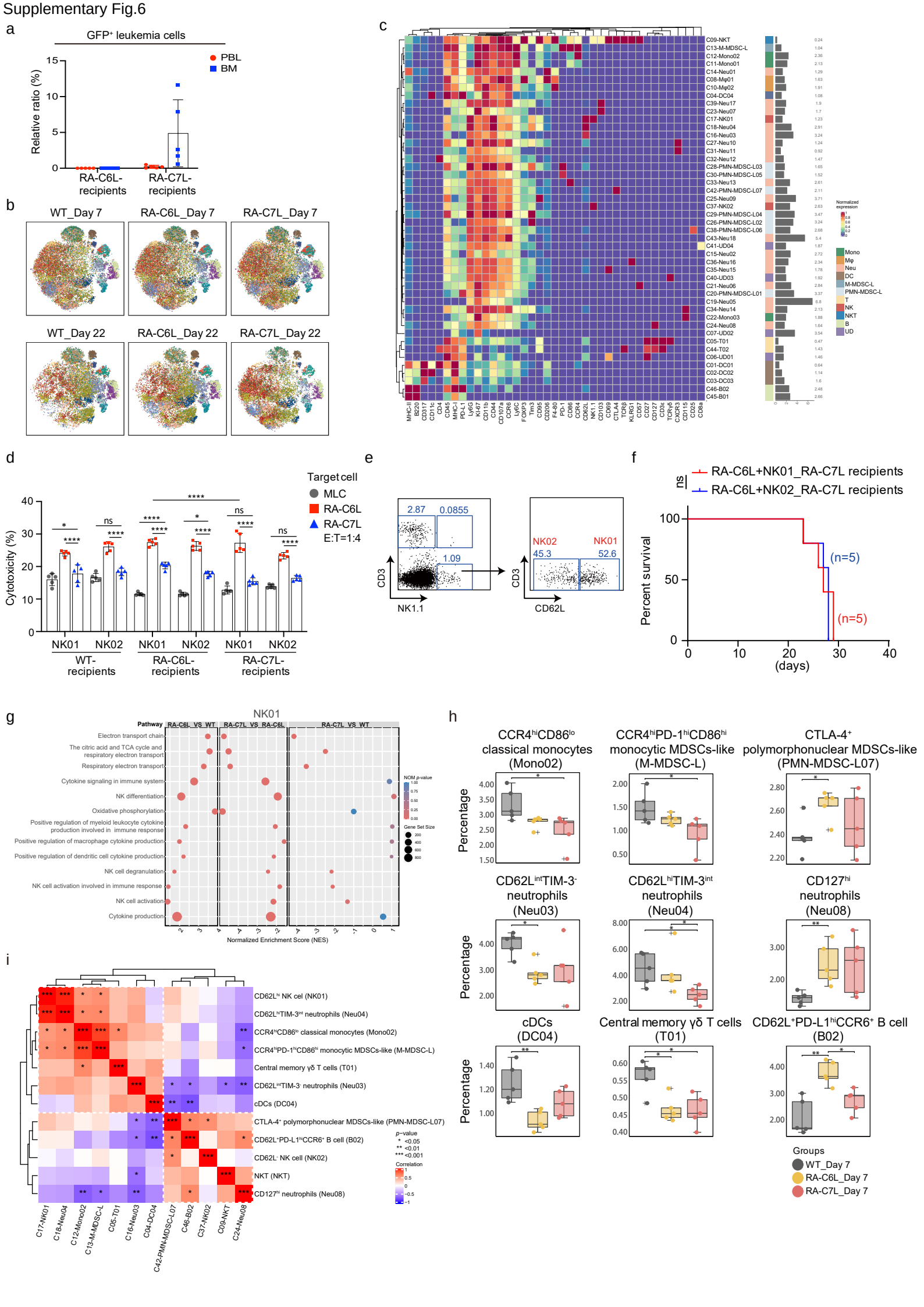

Supplementary Fig.6 Characterization of immune subsets responding to the inoculation of granulocytic LICs, related to Fig.6.

(**a**) 100 RA-C6L or RA-C7L cells as indicated were i.v. injected into unirradiated syngeneic mice on the day 0, and GFP^+ BM leukemic cells in the PBL and BM were analyzed using flow cytometry on the day 7 and day 22, respectively (n=5 for each group).

(**b**) t-SNE map displaying the compositions of immune cell subsets from different non-malignant bone marrow nucleated cells (BMMCs) samples as indicated.

(**c**) Heatmap showing normalized expression of 39 surface markers for 46 clusters identified with FlowSom. Relative frequencies are displayed as a bar graph to the right.

(**d**) Flow cytometric analysis of the *in vitro* cytotoxicity of the RA-PDC, RA-C6L, and RA-C7L cells towards NK01 and NK02 cells taken from the BM of three groups of mice (as shown in **Fig 6a**) on the day 7 (n=6 for each group).

(**e**) Flow cytometric detection of the relative distribution of NK01 and NK02.

(**f**) The survival curves of the FVB/NJ recipients intravenously implanted with 1000 RA-C6L cells and 5000 NK01 or NK02 cells. NK01 and NK02 cells were isolated from RA-C7L cells-inoculated recipients on the day 7 (n=5 for each group).

(**g**) GSEA of the enrichment profile of differentially expressed genes of the NK01 subsets taken from the WT mice or RA-C6L cell and RA-C7L cell-inoculated recipients.

(**h**) Boxplots showing the frequencies of the indicated immune subtypes across three groups of mice (n=5 for each group).

(**i**) Heatmap showing Spearman correlations of NK01 and NK02 with other immune subsets as indicated based on their frequency variations among individual mice of three groups (n=15) on the day 7.

Data are presented as mean ± SD. *p<0.05, **p<0.01, ***p<0.001. ns: not significant.